Comparison between traditional and competitive reaction models for the pyrolysis of high temperature aerospace materials

F. Torres Herrador [*], J. Coheur [†] and T. Magin [‡]
von Karman Institute for Fluid Dynamics, 1640, Rhode Saint Genese, Belgium,

J. Blondeau[§]
Vrije Universiteit Brussel, 1050, Brussels, Belgium

J. Meurisse[¶]
STC at NASA Ames Research Center, 94035, Moffett Field, California

F. Panerai[‖]
University of Illinois at Urbana-Champaign, IL 61801 Urbana, US

J. Lachaud[**]
Université de Bordeaux, 33405, Talence, France

N.N. Mansour[††]
NASA Ames Research Center, 94035, Moffett Field, California

When carbon/phenolic ablators used as spacecraft heatshields are submitted to high temperatures, they undergo a series of irreversible chemical reactions in a process known as pyrolysis. This process has been modeled using different approaches depending on the application field. We compare two pyrolysis models: the traditional devolatilization and the competitive reaction model commonly adopted in the analysis of biomass. We discuss advantages and disadvantages of each approach and provide results on the pyrolysis modeling of the Phenolic Impregnated Carbon Ablator using each method.

Nomenclature

0	Initial conditions	
β	Heating rate	$[\mathrm{K\,s^{-1}}]$
$\chi_{i,j}$	Advancement of the reaction	$[-]$
∞	Final conditions	
$\mathcal{A}_{i,j}$	Pre-exponential factor	$[-]$
$\mathcal{E}_{i,j}$	Activation Energy	$[\mathrm{kJ\,mol^{-1}}]$
$\mathcal{R}$	Universal gas constant	$[\mathrm{J\,K^{-1}\,mol^{-1}}]$

---

[*] PhD Candidate, Aeronautics and Aerospace Department, fratorhe@vki.ac.be
[†] PhD Candidate, Aeronautics and Aerospace Department, joffrey.coheur@vki.ac.be
[‡] Professor, Aeronautics and Aerospace Department, magin@vki.ac.be
[§] Professor, Thermo and Fluid dynamics (FLOW) Faculty of Engineering, jublonde@vub.ac.be
[¶] Research Scientist, Supercomputing Division, jeremie.b.meurisse@nasa.gov
[‖] Assistant Professor, Department of Aerospace Engineering, fpanerai@illinois.edu, Senior Member AIAA
[**] Research Scientist, Institute de Mécanique, jean.lachaud@u-bordeaux.fr, Senior Member AIAA
[††] Chief Division Scientist, Supercomputing Division, nagi.n.mansour@nasa.gov, Associate Fellow AIAA

$\mathcal{S}$	Solid	
c	Char material	
v	Virgin material	
π_{A_k}	Production rate of A_k	$[\mathrm{kg\,m^{-3}\,s^{-1}}]$
ρ	Density	$[\mathrm{kg\,m^{-3}}]$
$\tilde{F}_{i,j,k}$	Pseudo-F parameter	$[-]$
$\zeta_{i,j,k}$	Mass stoichiometric coefficient for devolatilization model	
ζ_s	Mass stoichiometric coefficient for competitive model	
A_k	Species k	
$F_{i,j}$	Fraction density loss of reaction j in phase i	$[-]$
k_r	Reaction Rate	
N_p	Number of solid phases	
$n_{i,j}$	Order of the reaction for devolatilization model	$[-]$
n_r	Order of the reaction for competitive model	$[-]$
P_i	Solid phases i in solid $\mathcal{S}$	
$R_{i,j}$	Reaction j in phase i	
T	Temperature	$[\mathrm{K}]$
amb	Ambient conditions	
DSC	Differential Scanning Calorimetry	
PATO	Porous material Analysis Toolbox based on OpenFOAM	
PICA	Phenolic Impregnated Carbon Ablator	
TACOT	Theoretical Ablative Composite for Open Testing	
TGA	Thermogravimetric Analysis	
TPS	Thermal Protection System	

I. Introduction

During atmospheric entry, the high kinetic energy of the spacecraft is converted into heat. The high temperatures achieved (~3000 K on the vehicle surface) require suitable Thermal Protection System (TPS) to protect the payload. In the recent years, a new generation of ablative TPS has gained attention due to their applicability to different entry scenarios. These materials are composites made up of carbon fibers bound together with a phenolic resin [1]. A good example of such material is the Phenolic Impregnated Carbon Ablator (PICA) developed by NASA, which has been successfully used in missions such as Mars Science Laboratory (MSL), and the Stardust Sample Return Capsule (SRC).

PICA features a great ablation performance due to several factors. The high porosity (80 %), which confers a low effective thermal conductivity, combined with high heat capacity of the components, reduce the heat flux towards the interior of the TPS. In addition, the phenolic resin undergoes an endothermic thermal degradation process known as pyrolysis. During this process, the polymeric chains break up, leading to a carbonaceous char and the release of gases [2]. These gases are of great importance since they are blown into the boundary layer generating an additional protection for the spacecraft [3]. An accurate prediction of the pyrolysis gases is required for a proper TPS design.

Several researchers have studied the thermal degradation of different phenolic composites. The first experimental studies were carried out in the 1960s by Golstein [4] and Sykes [5] on similar materials. In the late 1990s, Trick and Saliba [6, 7] developed the first kinetic model for the pyrolysis of a carbon/phenolic ablator. In these studies, the mass loss and the species produced were investigated by means of Thermogravimetric Analysis (TGA) and Gas Chromatography (GC). More recently, Lachaud *et al.* [8] developed a new pyrolysis model for PICA by compiling information from the aforementioned experiments. However, these studies were carried out at heating rates of $\beta \approx 20\,\mathrm{K\,min^{-1}}$, much lower than those experienced during actual atmospheric entry applications. Several studies [9, 10] have shown that the extrapolation of kinetic data towards higher heating rates may result in erroneous predictions of the material decomposition due to differences in the chemical reactions occurring. In fact, it has been shown [1, 11, 12] that the decomposition behavior of phenolic resin varies considerably as a function of heating rate. However, the current models used in the aerospace sector cannot reproduce such behavior. The thermal decomposition of the phenolic resin is similar to that of biomass [13, 14], which has different kinetic pathways under different heating conditions.

This can be explained by the degrees of freedom and the difference of time that the molecule chains have to break up and get released. In addition, the (competing) models developed for biomass pyrolysis seem appropriate to model the decomposition of phenolic. In this work, we first provide a brief review the state-of-the-art on the modeling of thermal degradation of solid materials. Then, we present results obtained applying the aforementioned models to the high temperature decomposition of PICA.

II. Modeling

Pyrolysis is a complex process which has been historically treated using different modeling approaches. Di Blasi [14] presents an extensive review of the different approaches. Among the different methods, there are two that have been most widely used: 1) devolatilization and 2) competitive reaction mechanisms. In the following, we describe the two methodologies from the physical description to the mathematical modeling highlighting pros and cons of each.

A. Devolatilization reaction mechanism

The devolatilization pyrolysis reaction mechanism (also referred to as parallel or multi-component mechanism) considers that a solid phase $\mathcal{S}$ is composed of N_p different sub-phases. Each phase P_i may be composed of N_{p_i} sub-phases $p_{i,j}$. A sub-phase $p_{i,j}$ undergoes a pyrolysis reaction that releases gases A_k in a proportion given by mass stoichiometric coefficients $\zeta_{i,j,k}$ (Fig. 1). The released mixture can be either treated as elements when equilibrium is used or as species when finite chemistry is used. The remaining solid after the completion of pyrolysis is known as char. This model can be generically formulated as:

$$\mathcal{S} \rightarrow \sum_{i}^{N_P} \sum_{j}^{N_{P_i}} p_{i,j}, \tag{1}$$

$$p_{i,j} \xrightarrow{R_{i,j}} \sum_{k}^{N_*} \zeta_{i,j,k} A_k, \quad * \begin{cases} e = \text{elements} \\ s = \text{species} \end{cases} \tag{2}$$

Each reaction $R_{i,j}$ is modeled using an Arrhenius-type equation, of the following form:

$$\frac{\mathrm{d}\chi_{i,j}}{\mathrm{d}t} = \mathcal{A}_{i,j}(1-\chi_{i,j})^{n_{i,j}} \exp\left(\frac{-\mathcal{E}_{i,j}}{\mathcal{R}T}\right), \tag{3}$$

where the advancement of reaction ($\chi_{i,j} \in [0,1]$) evolves as function of the kinetic parameters ($\mathcal{A}_{i,j}, \mathcal{E}_{i,j}, n_{i,j}$) and the temperature. The initial (or virgin) density of the solid is expressed as the sum of each sub-phase as:

$$\rho_{\mathrm{s,v}} = \sum_{i}^{N_P} \rho_{i,\mathrm{v}}. \tag{4}$$

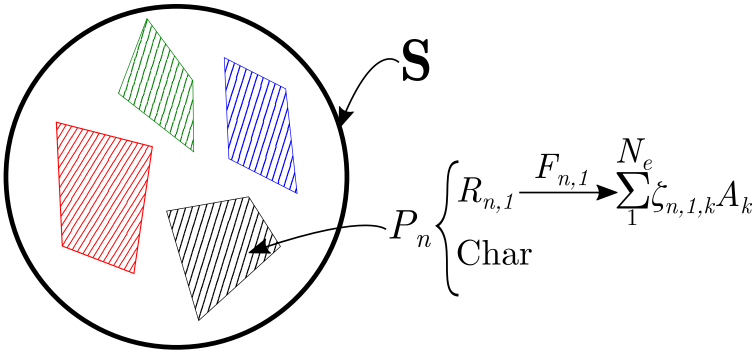

Fig. 1 Example of a Solid $\mathcal{S}$ made up of 4 sub-phases (colors). The sub-phase n (black) undergoes 1 pyrolysis step which produces a mass loss fraction $F_{n,1}$ and releases elements A_k given by $\zeta_{n,1,k}$.

The density evolution of the solid can be computed as the contribution of each advancement of reaction $\chi_{i,j}$ scaled by the density loss fraction $F_{i,j}$. This constant expresses the fraction of density that is lost when reaction $R_{i,j}$ reaches completion (i.e $\chi_{i,j} = 1$):

$$\rho_{\mathrm{s}}(t) = (\rho_{\mathrm{s,v}} - \sum_{i}^{N_P} \sum_{j}^{N_{R_i}} \rho_{i,\mathrm{v}} \chi_{i,j} F_{i,j}). \tag{5}$$

Similarly, the gas production rate of A_k (element or species) can be expressed as:

$$\pi_{A_k} = \sum_{i}^{N_P} \sum_{j}^{N_{R_i}} \rho_{i,\mathrm{v}} F_{i,j} \zeta_{i,j,k} \frac{\mathrm{d}\chi_{i,j}}{\mathrm{d}t}. \tag{6}$$

Using multicomponent volatilization mechanisms, one may assume that products which have production peaks at the same location, are produced by the same reaction and can thus be grouped.

Considering the devolatilization mechanism described, the production of each species A_k in the reaction $R_{i,j}$ can be assumed to be independent, and the use of stoichiometric coefficients can be replaced for k pyrolysis reactions which keep the same kinetic triplet ($\mathcal{A}_{i,j}$, $\mathcal{E}_{i,j}$, $n_{i,j}$), a weighted F parameter $\tilde{F}$ such that

$$\tilde{F}_{i,j,k} = \zeta_{i,j,k} F_{i,j}. \tag{7}$$

This allows to decouple the problem and removes the need of adding a unit sum constraint to the stoichiometric coefficient ($\sum_{k}^{N_*} \zeta_{i,j,k} = 1$), which could be a strong optimization constraint for reactions producing more than two gases. However, it can be seen that the final state and the amount of gases produced are pre-defined due to the use of the fraction loss mass $F_{i,j}$.

B. Competitive reaction mechanism

In competitive reaction mechanisms, a solid $\mathcal{S}_r$ can get decomposed into gases $\mathcal{G}_i$ and different new solids $\mathcal{S}_i$, which may further and further react in a chained process (Eq. 8). This model considers that the thermal decomposition of a solid can be described by the combination of different kinetic pathways. Indeed, the mechanism is so named by the fact that one reactant is generating different products at once, so that different kinetic pathways *compete* with each other to consume the reactant. Depending on the heating conditions, one pathway will be favored over others based on the different kinetic constants k_i. These different pathways allow to cover a broad range of heating conditions. A competitive mechanism on the solid phase $\mathcal{S}_r$ can be described as:

$$\mathcal{S}_r \xrightarrow{k_i} \zeta_i \mathcal{S}_i + (1 - \zeta_i) \mathcal{G}_i, \quad i \in N_{\text{product}}. \tag{8}$$

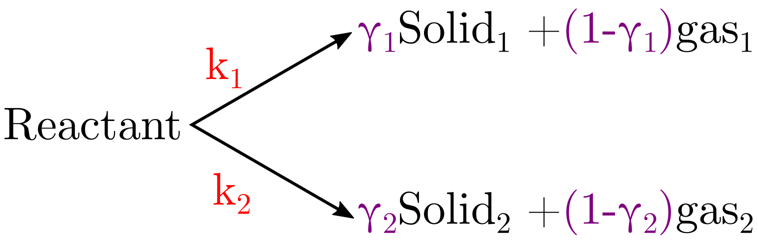

Fig. 2 Basic example of competing scheme: one reactant produces two different product plus two gases

A competitive scheme can be seen as a ramification tree. A solid component $\mathcal{S}_i$ in the tree may generated by its parents in the tree at a rate given by:

$$\frac{\mathrm{d}\rho_s}{\mathrm{d}t} = \sum_{r,s\neq reac} \zeta_s k_r \cdot \rho_{reac}^{n_r} \tag{9}$$

At the same time, the same solid $\mathcal{S}_i$ may be degraded into other solids or gases at a rate given by:

$$\frac{\mathrm{d}\rho_s}{\mathrm{d}t} = -\sum_{r,s=reac} k_r \cdot \rho_s^{n_r} \tag{10}$$

Thus, combining Eq. 9 and 10 provides the rate of production/destruction of a solid $\mathcal{S}_i$.

$$\frac{\mathrm{d}\rho_s}{\mathrm{d}t} = \underbrace{\sum_{r,s\neq reac} \zeta_s k_r \cdot \rho_{reac}^{n_r}}_{\text{generation term}} - \underbrace{\sum_{r,s=reac} k_r \cdot \rho_s^{n_r}}_{\text{destruction term}}, \tag{11}$$

where the reaction rate k_r is defined by the pre-exponential factor $\mathcal{A}$ and the activation energy $\mathcal{E}$:

$$k_r = \mathcal{A}_r \exp\left(\frac{-\mathcal{E}_r}{\mathcal{R}T}\right), \quad r \in N_r. \tag{12}$$

In Eq. 11, the order of the reaction n_r is commonly set to 1 in biomass applications in order to reduce the number of model parameters to be calibrated. In this model, the final state is not pre-defined since each pathway can generate different gases and/or char yields. However, their ability to predict gas yields at different heating conditions does not ensure extrapolation. The competitive model is developed for a range of specific conditions, and extrapolation outside such regime should be carefully studied [2].

Consideration of competitive reactions implies that a single density variable can be decomposed by several reaction rates, that are "in competition" with each other, as the reaction rate depends on temperature. We can also assume that a given density variable can become activated* and further reacts, leading to multi-step reactions with density variables that can be a function of each other. Intermediate variables start at zero density, become positive when they are created by another pyrolysis reaction and can ultimately go back to zero if consumed. With this assumption, it is therefore hard to express the problem in terms of a set of advancement coefficients since χ_i has to be monotonic to provide meaning to the advancement of a reaction. Some attempts have been made using the cumulative production of a given solid in the definition of the advancement coefficient [15]. Indeed, if an activated variable is consumed, then the advancement could go backward which would have no physical meaning. In addition, it is not possible to define the completion of a variable that starts at zero and is zero at the end of the pyrolysis process because it has been consumed.

As a basic illustration of a competitive mechanism reaction mechanism, let us consider a solid $\mathcal{S}$ which decomposes into two products, plus gases as shown in the schematic of Figure 2.

The system of equations can be expressed as follows:

---

*This is sometimes referred to as a depolimerization step [13].

Table 1 Kinetic constants

Reaction	1	2
log(A) (-)	2	11
E ($\mathrm{kJ\,mol^{-1}}$)	60	170
γ (-)	0.6	0.8

$$
\begin{aligned}
\frac{\mathrm{d}\rho_r}{\mathrm{d}t} &= -(k_1+k_2)\rho_r \\
\frac{\mathrm{d}\rho_{s1}}{\mathrm{d}t} &= \gamma_1 k_1 \rho_r \\
\frac{\mathrm{d}\rho_{s2}}{\mathrm{d}t} &= \gamma_2 k_2 \rho_r \\
\frac{\mathrm{d}\rho_{g1}}{\mathrm{d}t} &= (1-\gamma_1) k_1 \rho_r \\
\frac{\mathrm{d}\rho_{g2}}{\mathrm{d}t} &= (1-\gamma_2) k_2 \rho_r
\end{aligned} \tag{13}
$$

Let us also consider that *reaction 1* occurs at low temperatures and is slow, and that *reaction 2* occurs at higher temperatures, but it is fast.

We can also assume that the proportion of gases produced by *reaction 1* is higher than by *reaction 2.* For example: $\gamma_1 = 0.6$ and $\gamma_2 = 0.8$. The parameters chosen for this case are presented in Table 1.

We will simulate this case using four different heating rates $\beta = 0.5, 5, 50, 500\,\mathrm{K/min}$. Figure 3a presents the density loss for the different heating rates. The plot may suggest that *only* one pyrolysis *step* has occurred, however this is not the case. In Figure 3b, the evolution of the two products can be better observed. For slow heating rates ($\beta = 0.5\,\mathrm{K/min}$), *reaction 1* will have enough time to convert *Reactant* into $Solid_1$. As the heating rate is increased, *reaction 1* will not have enough time to consume the reactant before *reaction 2* gets active, and since it is much faster, it will consume reactant, generating $Solid_2$. It can be seen that the density of the *char* in Figure 3a is not a equal for the different simulated cases, but it is related to γ's and to the temporal evolution of the process (thus indirectly related to β).

This is a **key difference** of the competitive model compared to the parallel multi-component mechanisms when simulating the decomposition of phenolic resin [14]. Using parallel schemes, the final state is pre-defined by the F's associated to each pyrolysis reaction.

III. Comparative analysis of pyrolysis models

In this section, we show that the proposed multi-component, multi-step competitive reactions commonly used in the analysis of biomass pyrolysis [2, 13] are equivalent to the current devolatilization formulation of pyrolysis mechanism applied to the decomposition of pyrolyzing ablators [4, 8, 16]. They should be able to represent the same physics and we show that pyrolysis mechanisms used in TPS design ablation codes [17, 18] are actually a particular case of this generalized competitive scheme with single step and no competitive reactions.

Let's start from the general formulation of a decomposing solid following a single step and using the Šesták-Berggren kinetic model [19] for the advancement of reaction χ:

$$
\begin{aligned}
\frac{d\chi}{dt} &= f(\chi)k(T) \\
&= (1-\chi)^n \mathcal{A} \exp\left(-\frac{\mathcal{E}}{\mathcal{R}T}\right),
\end{aligned} \tag{14}
$$

where $\chi = \frac{\rho_0-\rho}{\rho_0-\rho_c}$. Eq. 14 is the classical formulation used for the pyrolysis of TPMs. It is assumed that several reactions $R_{i,j}$ are occurring independently from each other at different temperatures starting from

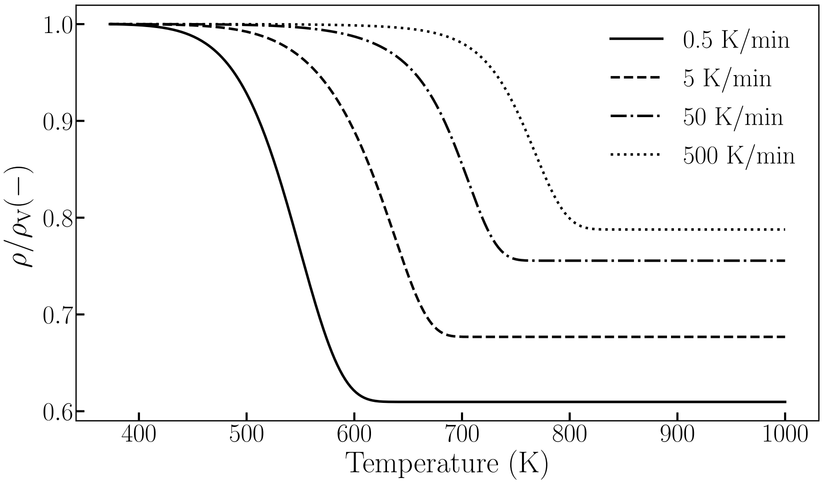

(a) Density loss of the reactant

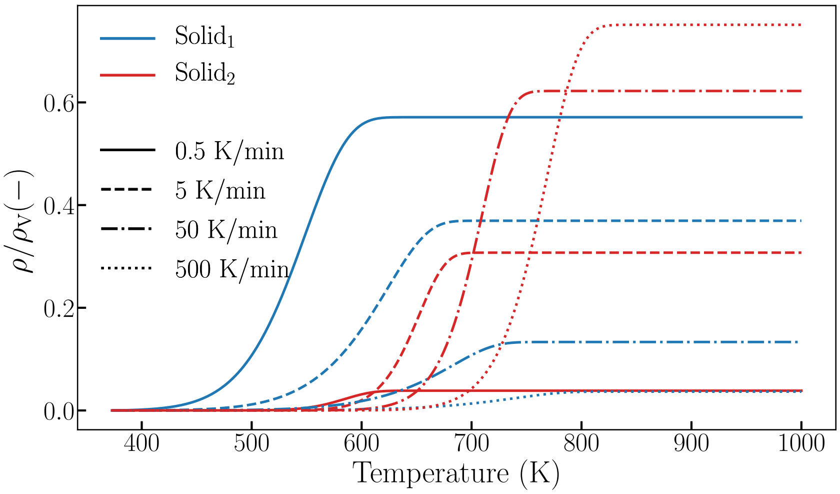

(b) Density evolution of the products

Fig. 3 Simulated results for 2 competing reactions with $\gamma_1 < \gamma_2$, for different heating rates β

an initial state ρ_0 until pyrolysis is completed and char material (ρ_c) is left. In terms of density variables, we have

$$\frac{d\rho}{dt} = -(\rho_0 - \rho_c)\left(\frac{\rho - \rho_c}{\rho_0 - \rho_c}\right)^n \mathcal{A}\exp\left(-\frac{\mathcal{E}}{\mathcal{R}T}\right). \tag{15}$$

In practice, neither the maximum (initial) values $\rho_{0,i}$, nor the char values $\rho_{c,i}$, are known a priori and it's not always possible to use Eq. 15 to express density variations. We use therefore the two following mathematical transformations to express the density variations. First, the constant $(\rho_0 - \rho_c)$ is incorporated in the pre-exponential factor $\mathcal{A}$ in order to have

$$\frac{d\rho}{dt} = -(\rho - \rho_c)^n \mathcal{A}' \exp\left(-\frac{\mathcal{E}}{\mathcal{R}T}\right), \tag{16}$$

where $\mathcal{A}'$ now has the unit of $\mathrm{s}^{-1}\ \mathrm{kg}^{-(n-1)}\ \mathrm{m}^{3(n-1)}$. Then, the reduced variable $\rho' \to \rho - \rho_c$ is introduced to remove the char component

$$\frac{d\rho'}{dt} = -(\rho')^n \mathcal{A}' \exp\left(-\frac{\mathcal{E}}{\mathcal{R}T}\right). \tag{17}$$

This formulation is equivalent to that presented in [2] for multi-component, single-step non-competitive reactions. To track the char evolution, it is now considered as a state variable ρ_c. The value for the advancement coefficient is now

$$\chi = \frac{\rho_0 - \rho}{\rho_0'}. \tag{18}$$

A. Linear multi-component, multi-step competitive reactions

Equation 17 for ρ' is for a single reaction with a single step. For competitive reactions with several dependent steps, and assuming linear reaction rates ($n = 1$), we can write the general matrix formulation

$$\frac{d\boldsymbol{\rho}}{dt} = \boldsymbol{A}(t)\boldsymbol{\rho} \tag{19}$$

where $\boldsymbol{A}(t)$ is a square matrix whose coefficients are obtained from the system of equations (see for example Eqs. 13) and are function of time. It is clear from Eq. 19 that a given density state variable ρ_i (either gas or solid), can be a function of all the other ones if the coefficient matrix $\boldsymbol{A}$ is full. When considering forward reactions only, due to the irreversibility of pyrolysis reactions, $\boldsymbol{A}$ is lower triangular (i.e. assuming no backward reactions, there can be no cycles in the reaction path). We are looking for a solution of the type

$$\boldsymbol{\rho}(t) = e^{\int_{t_0}^{t} \boldsymbol{A}(t)dt}\boldsymbol{\rho}_0 \tag{20}$$

which can be checked by differentiating it. In the simplest case where $\boldsymbol{A}$ is not a function of time, the solution of the system writes

$$\boldsymbol{\rho}(t) = e^{\boldsymbol{A}(t-t_0)}\boldsymbol{\rho}_0 \tag{21}$$

where the exponential of a given square matrix $\boldsymbol{X}$ is defined as

$$\exp(\boldsymbol{X}) = \sum_{k=0}^{\infty} \frac{1}{k!}\boldsymbol{X}^k. \tag{22}$$

This solution can be used for isotherm pyrolysis or a piecewiese constant heating rate as in the experiments of Wong *et al.*[20]. Practically, Eq. 21 can be computed using the spectral decomposition of $\boldsymbol{A}$ assuming it is diagonalizable with $\boldsymbol{A} = \boldsymbol{M}^{-1}\boldsymbol{\Lambda}\boldsymbol{M}$, where $\boldsymbol{M}$ is the matrix of eigenvectors and $\boldsymbol{\Lambda}$ is the diagonal matrix containing the eigenvalues $\boldsymbol{\Lambda} = \mathrm{diag}(\lambda_1, \lambda_2, \dots)$. Because $\boldsymbol{A}$ is constant, $\boldsymbol{M}$ is constant and we can write

$$\begin{aligned} \boldsymbol{\rho}(t) &= e^{\boldsymbol{M^{-1}\Lambda M}(t-t_0)}\boldsymbol{\rho}_0 && (23) \\ &= \boldsymbol{M^{-1}} e^{\boldsymbol{\Lambda}\Delta t}\boldsymbol{M}\boldsymbol{\rho}_0 && (24) \end{aligned}$$

where $e^{\boldsymbol{\Lambda}\Delta t} = \Delta t \mathrm{diag}(\lambda_1, \lambda_2, \dots)$. Initial conditions are $\boldsymbol{\rho_0} = (\rho_{\mathrm{init}}, 0, \dots, 0)^{\mathrm{T}}$, $\rho_c = 0$.

Considering now matrix $\boldsymbol{A}$ to be a function of time and looking for a solution of the type Eq. 20, we need to prove that $\boldsymbol{A}$ commutes with its integral $\int_{t_0}^{t} \boldsymbol{A}(t)dt$ for the exponential matrix to be valid [21]. Two matrices X and Y commute if $XY = YX$. There is no general condition or criterion for a matrix to commute with its integral [22]. We demonstrate here using a counterexample that the non constant coefficient matrix does not commute with its integral and so that a solution of the type Eq. 20 cannot be found. We consider the simple case of a two-step reaction mechanism $\rho_1 \to \rho_2 \to \rho_3$. The non-singular 2×2 coefficient matrix is $\boldsymbol{A} = \left(\begin{smallmatrix} -k_1 & 0 \\ k_1 & -k_2 \end{smallmatrix}\right)$ and $\boldsymbol{\rho} = (\rho_1, \rho_2)^{\mathrm{T}}$. It is worth noting that only the activated variables ρ_1 and ρ_2 need to be considered for the resolution of the system, as ρ_3 is a linear combination of the previous variables (ρ_3 can be obtained using mass conservation of the two reactants ρ_1 and ρ_2); considering ρ_3 in the system of PDEs would make the coefficient matrix singular. The two matrix products are

$$\boldsymbol{A}\boldsymbol{I_A} = \begin{pmatrix} k_1 I_1 & 0 \\ -k_1 I_1 - k_2 I_1 & k_2 I_2 \end{pmatrix}, \quad \boldsymbol{I_A}\boldsymbol{A} = \begin{pmatrix} k_1 I_1 & 0 \\ -k_1 I_1 - k_1 I_2 & k_2 I_2 \end{pmatrix}. \tag{25}$$

The condition for $\boldsymbol{A}$ to commute with $\boldsymbol{I_A}$ is $k_1 I_2 = k_2 I_1$. The result for $\boldsymbol{A}$ constant is immediately verified as we have $k_1 k_2 = k_2 k_1$. For the non constant case, we can show that the condition is

$$\exp\left(-\frac{\mathcal{E}_1}{RT}\right) \mathrm{Ei}\left(-\frac{\mathcal{E}_2}{RT}\right) = \exp\left(-\frac{\mathcal{E}_2}{RT}\right) \mathrm{Ei}\left(-\frac{\mathcal{E}_1}{RT}\right) \tag{26}$$

(where Ei is the exponential integral function) cannot be verified. As a conclusion, when considering multi-step non isotherm reactions, an analytical solution of the form of Eq. 20 will generally not be found.

Finally, we consider the most general case of multi-component multi-steps competitive reactions. For this general case, we can again use the matrix formalism of Eq. 19 where now

$$\boldsymbol{A} = \begin{pmatrix} M_1 & 0 & \cdots & 0 \\ 0 & M_2 & \cdots & 0 \\ \vdots & \vdots & \ddots & \vdots \\ 0 & 0 & \cdots & M_n \end{pmatrix} \tag{27}$$

is a block diagonal matrix. Each block M_i is a lower triangular square matrix of different dimension n_i representing a particular component of the pyrolysis mechanism. The null entries represent matrices which dimensions are consistent with the block diagonal. Each block is decoupled and can be solved separately. The generalized initial conditions are now

$$\boldsymbol{\rho_0} = (\underbrace{\rho_{1,\mathrm{init}}, 0, \dots, 0}_{n_1}, \underbrace{\rho_{2,\mathrm{init}}, 0, \dots, 0}_{n_2}, \dots, \underbrace{\rho_{n,\mathrm{init}}, 0, \dots, 0}_{n_n})^{\mathrm{T}}. \tag{28}$$

The previous case of pyrolysis reactions for aerospace applications was in fact considering 1×1 matrices $M_i = k_i$ with $\boldsymbol{\rho_0} = (\rho_{1,\mathrm{init}}, \rho_{2,\mathrm{init}}, \dots)^{\mathrm{T}}$ and is therefore a particular case of this general formulation. For this case, because $\boldsymbol{A}$ is diagonal it commutes with its integral and it is possible to find an analytical solution of the form of Eq. 20. It was also possible to find a closed form of the solution for the non-linear system of PDEs, both for $\boldsymbol{A}$ constant and for linear heating rates.

In summary, we have shown that the pyrolysis mechanisms widely adopted to model ablators are a particular case of the general multi-component, single-step competitive reactions when considering first order reactions. For these models, the coefficient matrix is diagonal, leading to uncoupled system of PDEs for which we can find analytical solutions under both isotherm and linear heating rate pyrolysis. Using the general model formulation can therefore help to predict more complex pyrolysis phenomena, for example the shift in production curves with the increase of the heating rate [2]. However, in most of the cases, a direct comparison between devolatilization and competitive mechanisms will not be possible.

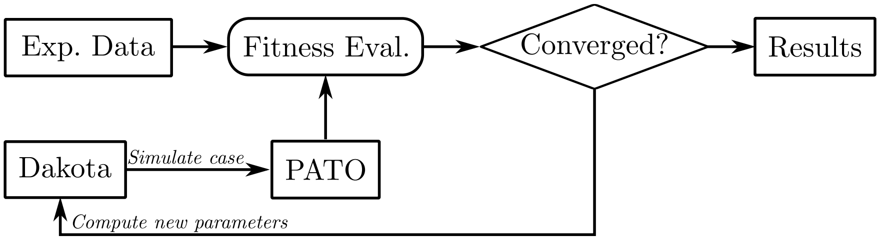

Fig. 4 Basic structure of the optimization setup.

IV. Calibration methodology

The model parameters presented in Section II can be fitted to reproduce data from controlled laboratory experiments. The basic structure of the calibration methodology has been essentially the same in the different models presented and it is depicted in Figure 4 [23]. We use the optimization tool Dakota [24] developed by Sandia National Laboratories to calibrate the model parameters. At each iteration of the optimization process, Dakota sets up the appropriate parameters for the pyrolysis mechanism. With those parameters, the numerical solver Porous material Analysis Toolbox based on OpenFOAM (PATO) developed by Lachaud *et al.* [8] performs a simulation of the pyrolysis process with the given conditions of heating rate, geometry (commonly 0D), material properties, etc.

The soft coupling between PATO and Dakota allows notable flexibility. It permits evaluating a large variety of optimization methods (e.g. gradient based and evolutionary), and allows to choose which model (multicomponent, competing, etc.) or level of fidelity is desired to simulate the solid thermal decomposition in PATO.

V. Results

Hereafter, we present results for both devolatilization and competitive mechanisms derived from experimental data. For the competitive mechanism, we use experimental results on the pyrolysis decomposition of PICA by Bessire and Minton [25]. For the competitive, we combined two independent sets of PICA data: the aforementioned data by Bessire and Minton [25] at high heating rate, and measurements by Wong *et al.* [20], at low heating rate.

A. A high heating rate elemental model for PICA

We first summarize results that are presented in greater detail in our recent work [23]. Bessire and Minton [25] carried out Mass Spectroscopy (MS) experiments using PICA samples, in which 14 significant pyrolysis products were identified. These products are organic compounds of the form $C_xH_yO_z$, therefore one can then consider the elemental (C, H and O) contributions of each compound to construct a finite rate elemental model for PICA. If required, the species composition may be obtained assuming chemical equilibrium.

The proposed devolatilization scheme consists of 4 parallel reactions [4, 5, 8] in which C, H and O are released following stoichiometric coefficients $\zeta_{j,k}$.

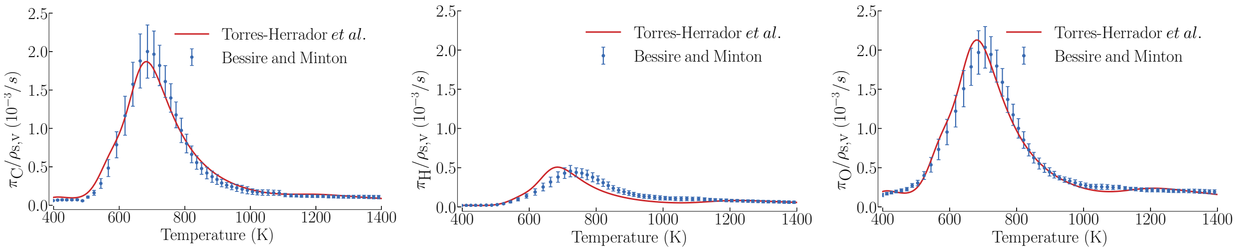

(a) Carbon **(b) Hydrogen** **(c) Oxygen**

Fig. 5 Results from the parameter calibration. Simulations (—) show good agreement with Experiments (●). The error-bars represent 1σ experimental uncertainty.

In addition, the mass loss evolution can be obtained by integrating the element production rates as shown in Figure 6 also presenting great agreement with the results by Bessire and Minton.

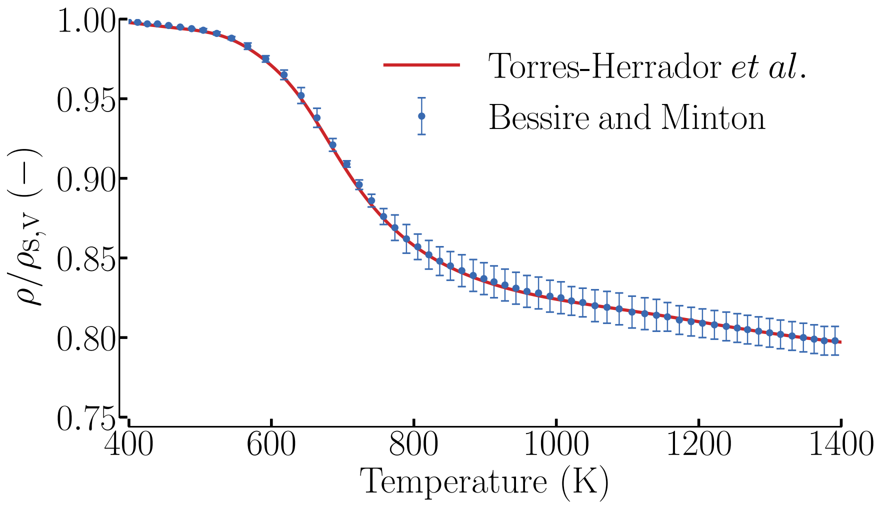

Fig. 6 Reconstructed TGA curve from the element production rate.

B. A first competitive mechanism for PICA

In this section, we present the development of a preliminary competitive scheme for PICA using experimental data from two different sources [20, 25]. These data were collected at two distinct heating rates, $\beta = 10\ \mathrm{K\,min^{-1}}$[20] and $\beta = 366\ \mathrm{K\,min^{-1}}$[25] respectively. It can be observed (Fig 8a) that at high heating rates, the decomposition curve shifts towards lower temperatures, contrary to common TGA measurements. This behavior was already observed in the past with the work of Stokes [12] or Jackson and Conley [11] and is analyzed in details in [25].

We consider a phenomenological approach based on the measured density loss. The proposed scheme is shown in Figure 7. The different values for the kinetic constant determine the predominant path at the two different heating rates. At low heating rate conditions, the process spends a considerable amount of time converting the Reactant into an intermediate state called Activation$_{\mathrm{slow}}$, which further reacts into Solid 1 and releases gas 1. At high heating rate conditions, k_1 does not have enough time to produce Activation$_{\mathrm{slow}}$ because k_3 is a much faster process, thus producing Activation$_{\mathrm{fast}}$. This path leads to a higher production of Solid 2 and gas 2. These results can be observed in Figure 9.

Notably, this approach allows to retrieve the density loss at both heating rates as depicted in Figure 8. In order to keep improving the proposed scheme, additional data at intermediate heating rates is required.

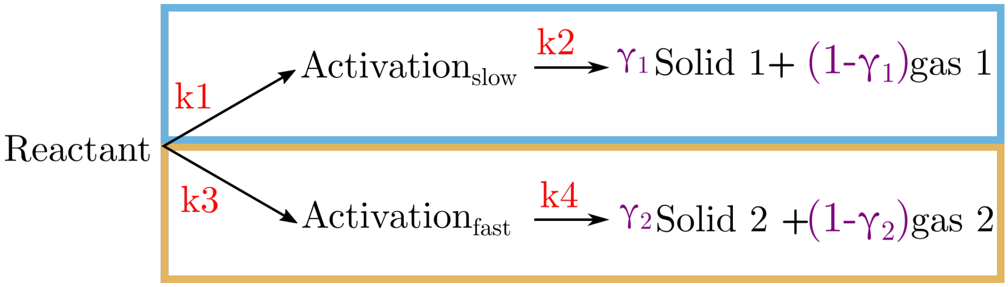

Fig. 7 Proposed competitive scheme for the pyrolysis of SC1008 resin.

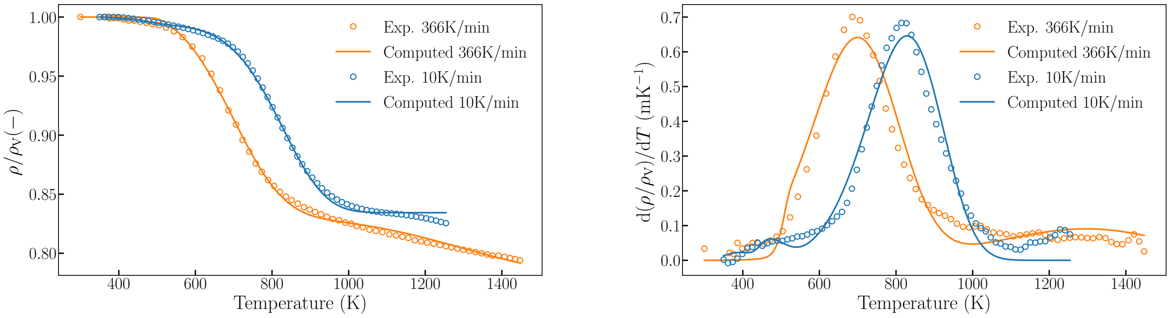

(a) Density loss **(b) Density loss rate**

Fig. 8 Competitive pyrolysis calibration results for PICA.

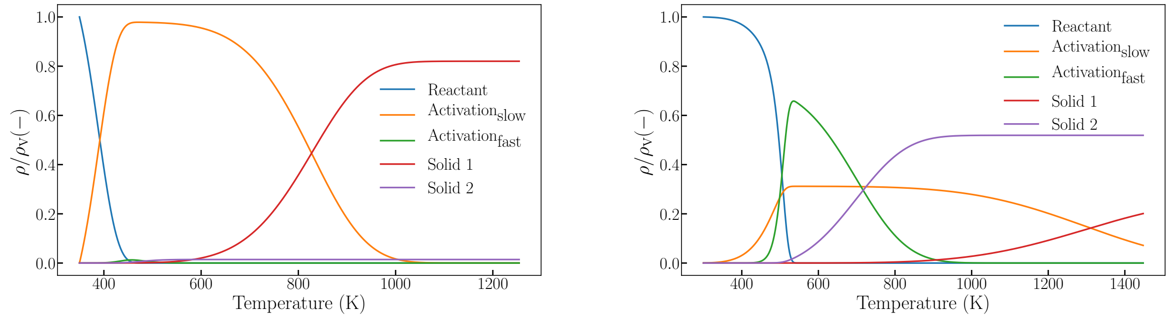

(a) 10 K min^{-1} **(b)** 366 K min^{-1}

Fig. 9 Production/Destruction rates of the different solids.

VI. Conclusions

In summary, we have revised two different approaches to model the pyrolysis process: the devolatilization model currently used in the aerospace sector, and the competitive reaction model commonly applied in biomass.

The devolatilization model assumes that reactions occur in parallel without any kind of interactions between the sub-phases. This allows to fully decouple the problem and be able to compute analytical solutions in most of the cases. This model has shown good agreement with experimental data at a given condition of heating rate. However, recent experimental findings show that this model is not capable of reproducing the complexity of the pyrolysis process at largely varying heating rates.

The alternative scheme proposed in this paper aims to use the competitive mechanisms. In this model, a reactant can take different kinetic paths depending on the time evolution of the environment conditions and location within a material sample. Our results show that we are now capable of capturing major pyrolysis features occurring at two heating rates differing by more than an order of magnitude. Building upon the presented analysis, we anticipate further investigations on pyrolysis modeling based on competitive reactions for the decomposition of phenolic resin. Additional data that resolves a broad range of heating rates is also needed to assess the validity of the proposed scheme and improve it.

Acknowledgments

The research of F. Torres Herrador is supported by SB PhD fellowship 1S58718N of the Research Foundation Flanders (FWO).

This work is supported by the Entry Systems Modeling project (M. J. Wright project manager, M. D. Barnhardt principal investigator) as part of the NASA Game Changing Development program.

The authors would like to acknowledge Dr. Brody Bessire for the useful discussions and comments on this work.

References

[1] Bessire, B. K., Lahankar, S. A., and Minton, T. K., "Pyrolysis of Phenolic Impregnated Carbon Ablator (PICA)," *ACS Applied Materials & Interfaces*, Vol. 7, No. 3, 2015, pp. 1383–1395. doi:10/f62x9w, URL `https://doi.org/10.1021/am507816f`.

[2] Blondeau, J., and Jeanmart, H., "Biomass pyrolysis at high temperatures: Prediction of gaseous species yields from an anisotropic particle," *Biomass and Bioenergy*, Vol. 41, 2012, pp. 107–121. doi:10/f3zmcx, URL `http://www.sciencedirect.com/science/article/pii/S0961953412001043`.

[3] Duffa, G., *Ablative Thermal Protection Systems Modeling*, American Institute of Aeronautics and Astronautics, Publisher, 2013.

[4] Goldstein, H. E., "Pyrolysis Kinetics of Nylon 6–6, Phenolic Resin, and Their Composites," *Journal of Macromolecular Science: Part A - Chemistry*, Vol. 3, No. 4, 1969, pp. 649–673. doi:10.1080/10601326908053834, URL `http://dx.doi.org/10.1080/10601326908053834`.

[5] Sykes, G. F., "Decomposition Characteristics of a Char-Forming Phenolic Polymer Used for Ablative Composites." Tech. Rep. TN D-3810, 1967.

[6] Trick, K. A., and Saliba, T. E., "Mechanisms of the pyrolysis of phenolic resin in a carbon/phenolic composite," *Carbon*, Vol. 33, No. 11, 1995, pp. 1509–1515. doi:10.1016/0008-6223(95)00092-R, URL `http://www.sciencedirect.com/science/article/pii/000862239500092R`.

[7] Trick, K. A., Saliba, T. E., and Sandhu, S. S., "A kinetic model of the pyrolysis of phenolic resin in a carbon/phenolic composite," *Carbon*, Vol. 35, No. 3, 1997, pp. 393–401. doi:10.1016/S0008-6223(97)89610-8, URL `http://www.sciencedirect.com/science/article/pii/S0008622397896108`.

[8] Lachaud, J., Scoggins, J. B., Magin, T. E., Meyer, M. G., and Mansour, N. N., "A generic local thermal equilibrium model for porous reactive materials submitted to high temperatures," *International Journal of Heat and Mass Transfer*, Vol. 108, Part B, 2017, pp. 1406–1417. doi:10.1016/j.ijheatmasstransfer.2016.11.067.

[9] Agarwal, R. K., "On the use of the arrhenius equation to describe cellulose and wood pyrolysis," *Thermochimica Acta*, Vol. 91, 1985, pp. 343–349. doi:10/fr8tn3, URL `http://www.sciencedirect.com/science/article/pii/0040603185852278`.

[10] Šimon, P., "Isoconversional methods," *Journal of Thermal Analysis and Calorimetry*, Vol. 76, No. 1, 2004, p. 123. doi:10/bmrvgn, URL `https://link.springer.com/article/10.1023/B:JTAN.0000027811.80036.6c`.

[11] Jackson, W. M., and Conley, R. T., "High temperature oxidative degradation of phenol–formaldehyde polycondensates," *Journal of Applied Polymer Science*, Vol. 8, No. 5, 1964, pp. 2163–2193. doi:10/cbfhmp, URL `https://onlinelibrary.wiley.com/doi/abs/10.1002/app.1964.070080516`.

[12] Stokes, E. H., "Kinetics of pyrolysis mass loss from cured phenolic resin," *Journal of Thermophysics and Heat Transfer*, Vol. 9, No. 2, 1995, pp. 352–358. doi:10.2514/3.667, URL `https://doi.org/10.2514/3.667`.

[13] Miller, R. S., and Bellan, J., "A Generalized Biomass Pyrolysis Model Based on Superimposed Cellulose, Hemicelluloseand Liqnin Kinetics," *Combustion Science and Technology*, Vol. 126, No. 1-6, 1997, pp. 97–137. doi:10.1080/00102209708935670.

[14] Di Blasi, C., "Modeling chemical and physical processes of wood and biomass pyrolysis," *Progress in Energy and Combustion Science*, Vol. 34, No. 1, 2008, pp. 47–90. doi:10/cszkrc, URL `http://www.sciencedirect.com/science/article/pii/S0360128507000214`.

[15] Lautenberger, C., and Fernandez-Pello, A. C., "Optimization Algorithms for Material Pyrolysis Property Estimation," *Fire Safety Science*, Vol. 10, 2011, pp. 751–764. URL `http://www.iafss.org/publications/fss/10/751`.

[16] Coheur, J., Turchi, A., Schrooyen, P., and Magin, T., "Development of a unified model for flow-material interaction applied to porous charring ablators," *47th AIAA Thermophysics Conference*, Denver, Colorado, 2017. doi:10.2514/6.2017-3684.

[17] Omidy, A. D., Panerai, F., Martin, A., Lachaud, J., Cozmuta, I., and Mansour, N. N., "Code-to-Code Comparison, and Material Response Modeling of Stardust and MSL using PATO and FIAT," Technical Report NASA/CR-2015-218960, NASA Ames Research Center, Jun. 2015. URL `https://ntrs.nasa.gov/search.jsp?R=20160006963`.

[18] Amar, A. J., Olivier, A. B., Kirk, B. S., Salazar, G., and Droba, J., "Overview of the CHarring Ablator Response (CHAR) Code," Washington, DC, United States, 2016. URL `https://ntrs.nasa.gov/search.jsp?R=20160005889`.

[19] Málek, J., and Criado, J. M., "Empirical kinetic models in thermal analysis," *Thermochimica Acta*, Vol. 203, 1992, pp. 25–30. doi:10/bfg7ms.

[20] Wong, H.-W., Peck, J., Assif, J., Panerai, F., Lachaud, J., and Mansour, N. N., "Detailed analysis of species production from the pyrolysis of the Phenolic Impregnated Carbon Ablator," *Journal of Analytical and Applied Pyrolysis*, Vol. 122, 2016, pp. 258–267. doi:10/f9h46d, URL `http://www.sciencedirect.com/science/article/pii/S016523701630211X`.

[21] Nemytskii, V. V., Stepanov, V. V., and Stepanov, V. V., *Qualitative Theory of Differential Equations*, Courier Corporation, 1989.

[22] Epstein, I. J., "Conditions for a Matrix to Commute with its Integral," *Proceedings of the American Mathematical Society*, Vol. 14, No. 2, 1963, pp. 266–270. doi:10/bpwd8w, URL `https://www.jstor.org/stable/2034625`.

[23] Torres Herrador, F., Meurisse, J. B. E., Panerai, F., Blondeau, J., Lachaud, J., Bessire, B. K., Magin, T. E., and Mansour, N. N., "A high heating rate pyrolysis model for the Phenolic Impregnated Carbon Ablator (PICA) based on mass spectroscopy experiments," *Journal of Analytical and Applied Pyrolysis*, Vol. Manuscript sumbitted for publication, 2019.

[24] Adams, B. M., Bauman, L., Bohnhoff, W. J., Dalbey, K. R., Ebeida, M., Eddy, J. P., Eldred, M. S., Hough, P., Hu, K., Jakeman, J., Stephens, J., Swiler, L. P., Vigil, D., and Wildey, T., "DAKOTA : a multilevel parallel object-oriented framework for design optimization, parameter estimation, uncertainty quantification, and sensitivity analysis. Version 6.7, user's reference manual." Tech. Rep. SAND2014-4633, Sandia National Laboratories, Nov. 2017. doi:10.2172/991841.

[25] Bessire, B. K., and Minton, T. K., "Decomposition of Phenolic Impregnated Carbon Ablator (PICA) as a Function of Temperature and Heating Rate," *ACS Applied Materials & Interfaces*, Vol. 9, No. 25, 2017, pp. 21422–21437. doi:10.1021/acsami.7b03919, URL `http://dx.doi.org/10.1021/acsami.7b03919`.